Journal of Japan Association for Earthquake Engineering, Vol.15, No.2, 2015

NUMERICAL DERIVATIONS OF A MACROSCOPIC MODEL FOR REINFORCED CONCRETE WALLS CONSIDERING IN-PLANE AND OUT-OF-PLANE BEHAVIOR

Panon LATCHAROTE[1] and Yoshiro KAI[2]

[1] Graduate Student, Dept. of Infrastructure Systems Eng., Kochi University of Technology, Kochi, Japan, panoname@hotmail.com
[2] Member of JAEE, Professor, Dept. of Infrastructure Systems Eng., Kochi University of Technology, Kochi, Japan, kai.yoshiro@kochi-tech.ac.jp

ABSTRACT: A macroscopic model, macro plate model, was proposed to represent a wall member of RC walls. Both in-plane and out-of-plane behavior were considered for numerical derivations of macro plate model. For out-of-plane behavior, bending deformation was incorporated with shear deformation to consider out-of-plane deformation as same as in-plane behavior. The hysteretic behavior of macro plate model can be directly expressed by stress-strain relationships in any conventional hysteretic rules, which have been proposed by other researchers, for member level. Unless nonlinear analysis of RC walls was proposed in case of earthquake, macro plate model can be proposed for nonlinear analysis of those in case of wind and tsunami by converting distributed force to nodal force.

Key Words: macro plate model, RC walls, in-plane, out-of-plane, distributed force

1. INTRODUCTION

In RC buildings, RC walls are widely used to increase resistance against lateral loads imposed by earthquake, wind, and tsunami. For such buildings, RC walls and beam-column frames are combined in nonlinear structural analysis, so a proper modeling of RC walls is very important for structural engineering applications. Many analytical models have been proposed for nonlinear analysis of RC walls. These analytical models are classified as microscopic and macroscopic models, representing local and overall behavior of RC walls respectively. For microscopic models, finite element model (FEM) is conducted to predict local behavior of RC walls using a constitutive model of materials. On the other hand, various macroscopic models have been proposed for RC walls verified with experimental results and these macroscopic models can be used practically for wall-frame structural analysis. These macroscopic models in Fig. 1, such as the three-vertical-line element model (TVLEM proposed by Kabeyasawa et al., 1983), the multi-vertical-line element model (MVLEM proposed by Volcano et al., 1988), the 2-D nonlinear plane element model (Milev, 1996), and the iso-parametric element model (IPEM proposed by Chen et al., 2000), have been proposed for modeling RC walls. Due to state-of-the-art constitutive models and less computation time, macroscopic models are more

practical and efficient than microscopic models for structural engineering applications. However, macroscopic models have been developed based on a simplifier idealization and restricted validity upon derivation models. In addition, only in-plane behavior of RC walls have been studied in these macroscopic models.

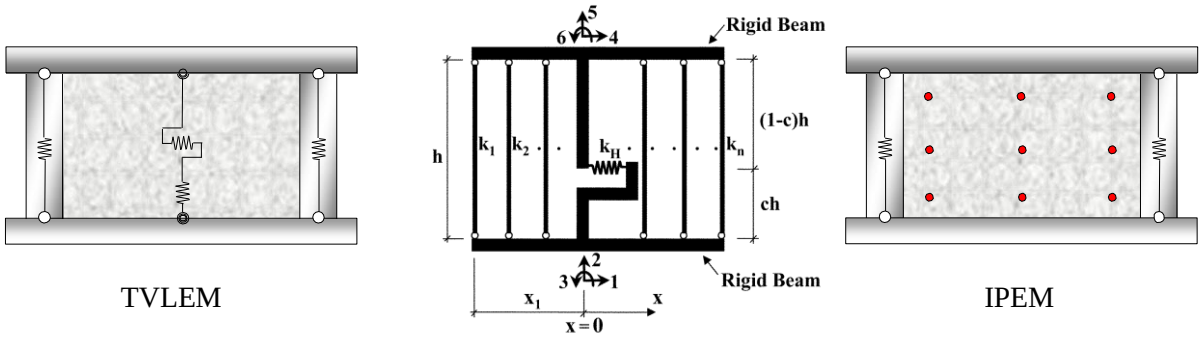

Fig. 1 Macroscopic models

This study proposes macro plate model, a macroscopic model representing a wall member of RC walls. Macro plate model was a four-node element model which was developed originally from the theory of elasticity (Timoshenko et al., 1970) for in-plane behavior and the theory of plate bending (Zienkiewicz et al., 2005) for out-of-plane behavior. Since macro plate model was developed from elastic theory of plate element, stress-strain relationships in macro plate model was derived to simulate inelastic response of RC walls using hysteretic stress-strain relationships in hysteretic rules, which have been proposed by other researchers.

2. DESCRIPTION OF A PROPOSED MACROSCOPIC MODEL

Macro plate model, a proposed macroscopic model for a wall member of RC walls, was a four-node element with rectangular shape in the x-y plane, consisting of nodes i, j, k, and l shown in Fig. 2(a). The entire wall member was modeled as a rectangular plane member assuming uniform concrete plate and uniformly orthogonal bar arrangement in order to consider in-plane and out-of-plane behavior. The origin of the coordinate system was on the center of macro plate model. For the dimensions of macro plate model, l_x and l_y were defined as the length of a wall member and thickness t was constant within each wall member. As shown in Fig. 2(b), macro plate model was formulated to describe a one-story wall member of RC walls.

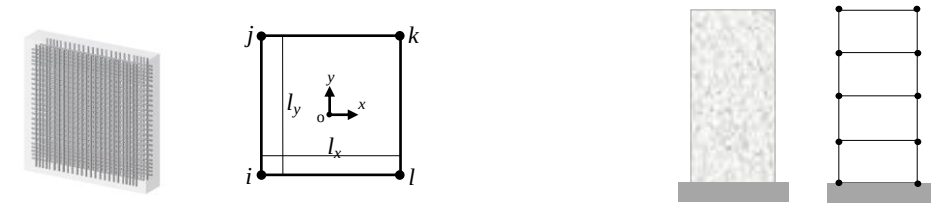

Fig. 2 Macro plate model

For each node of macro plate model, a total of five degrees of freedoms were considered: three translational components along the x-, y-, and z-axes and two rotational components about the x- and y-axes. Of these, macro plate model had twenty degrees of freedom, in which eight components were defined as in-plane degrees of freedom and twelve as out-of—plane degrees of freedom in Fig. 3.

In-plane and out-of-plane displacement of nodes i, j, k, and l are shown in Fig. 3(a) and Fig. 3(b) respectively. As can be seen in Fig. 3(a), two translational displacements along the x- and y- axes (u and v) were assigned to nodes i, j, k, and l, whereas one translational displacement along the z-axis (w) and two rotational displacements around the x- and y-axes (θ_x and θ_y) were assigned to nodes i, j, k, and l shown Fig. 3(b).

(a) DOFs of in-plane displacement (b) DOFs of out-of-plane displacement

Fig. 3 Degree of freedoms (DOFs) of macro plate model

3. IN-PLANE BEHAVIOR OF MACRO PLATE MODEL

As aforementioned above, in-plane behavior of macro plate model was derived originally from the theory of elasticity using the plane-sections-remain-plane assumption. Axial deformation in the x- and y-directions (δ_x and δ_y), in-plane bending deformation in the x-y plane (τ_x and τ_y), and in-plane shear deformation in the x-y plane (τ_0) are expressed in Fig. 4(a), Fig. 4(b), and Fig. 4(c) respectively.

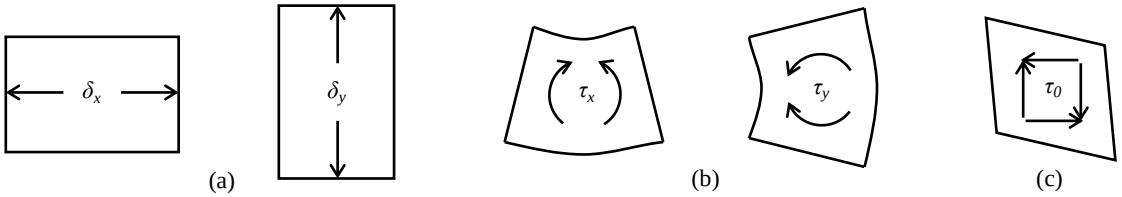

Fig. 4 (a) Axial deformation, (b) Bending deformation, and (c) Shear deformation

In relation with in-plane deformation, axial forces in the x- and y-directions (N_x and N_y), in-plane bending moments in the x-y plane (M_x and M_y), anti-symmetric in-plane bending moment in the x-y plane (M_0) are expressed in Fig. 5(a), Fig. 5(b), and Fig. 5(c) respectively.

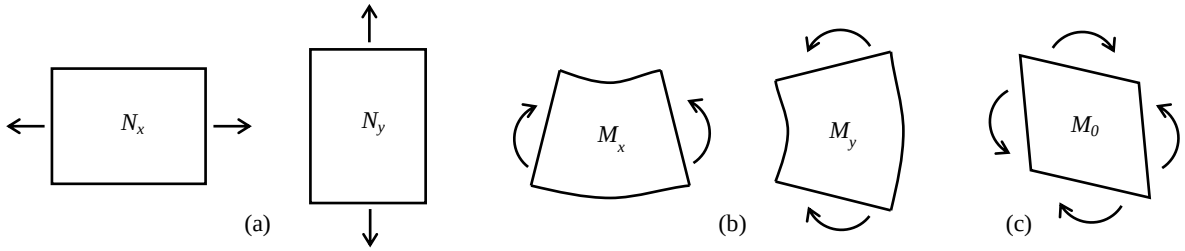

Fig. 5 (a) Axial force, (b) Bending moment, and (c) Anti-symmetric bending moment

For in-plane behavior, in-plane deformation in Fig. 4 is expressed in term of in-plane displacement in Fig. 3(a) as Eq. (1) and the stiffness matrix were derived based on the theory of elasticity (Timoshenko et al., 1970) as Eq. (1).

$$\begin{bmatrix}\delta_x\\ \delta_y\\ \tau_x\\ \tau_y\\ \tau_0\end{bmatrix}=\begin{bmatrix}-\frac{1}{2} & 0 & -\frac{1}{2} & 0 & \frac{1}{2} & 0 & \frac{1}{2} & 0\\ 0 & -\frac{1}{2} & 0 & \frac{1}{2} & 0 & \frac{1}{2} & 0 & -\frac{1}{2}\\ -\frac{1}{l_y} & 0 & \frac{1}{l_y} & 0 & -\frac{1}{l_y} & 0 & \frac{1}{l_y} & 0\\ 0 & \frac{1}{l_x} & 0 & -\frac{1}{l_x} & 0 & \frac{1}{l_x} & 0 & -\frac{1}{l_x}\\ \frac{1}{2l_y} & \frac{1}{2l_x} & -\frac{1}{2l_y} & \frac{1}{2l_x} & -\frac{1}{2l_y} & -\frac{1}{2l_x} & \frac{1}{2l_y} & -\frac{1}{2l_x}\end{bmatrix}\begin{bmatrix}u_i\\ v_i\\ u_j\\ v_j\\ u_k\\ v_k\\ u_l\\ v_l\end{bmatrix}\quad\begin{bmatrix}N_x\\ N_y\\ M_x\\ M_y\\ M_0\end{bmatrix}=\begin{bmatrix}\frac{1}{1-\nu^2}\frac{EA_x}{l_x} & \frac{\nu}{1-\nu^2}\frac{EA_x}{l_y} & 0 & 0 & 0\\ \frac{\nu}{1-\nu^2}\frac{EA_y}{l_x} & \frac{1}{1-\nu^2}\frac{EA_y}{l_y} & 0 & 0 & 0\\ 0 & 0 & \frac{EI_x}{l_x} & 0 & 0\\ 0 & 0 & 0 & \frac{EI_y}{l_y} & 0\\ 0 & 0 & 0 & 0 & \frac{1}{\frac{\kappa}{Gtl_xl_y}+\frac{l_x}{12EI_x'}+\frac{l_y}{12EI_y'}}\end{bmatrix}\begin{bmatrix}\delta_x\\ \delta_y\\ \tau_x\\ \tau_y\\ \tau_0\end{bmatrix}\qquad(1)$$

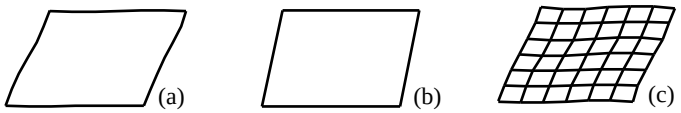

Fig. 6 (a) Macro plate model, (b) A four-node element of FEM, and (c) A wall member of FEM

Anti-symmetric in-plane bending deformation of macro plate model is shown in Fig. 6(a). The effect of in-plane shear deformation was incorporated as shown in the last row of stiffness matrix in Eq. (1), whereas anti-symmetric in-plane bending deformation is usually not considered in a four-node element of FEM shown in Fig. 6(b). Therefore, a wall member of FEM is finely divided to consider the effect of anti-symmetric in-plane bending deformation by axial deformation of each divided element shown in Fig. 6(c).

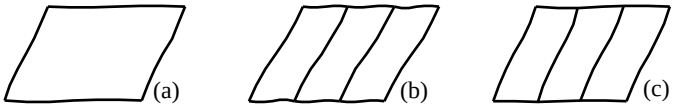

Fig. 7 In-plane deformation of macro plate model

As shown in Fig. 7(a), macro plate_model can obtain high accuracy solution with large element division. If a wall member was modeled with several elements of macro plate model, anti-symmetric in-plane bending deformation of individual elements occurred independently instead of entire deformation of a wall member shown in Fig. 7(b). However, the entire deformation shown in Fig. 7(c) can be obtained by using I_x' instead of I_x at the last row of stiffness matrix in Eq. (1) in which I_x' can be calculated by full length of a wall member.

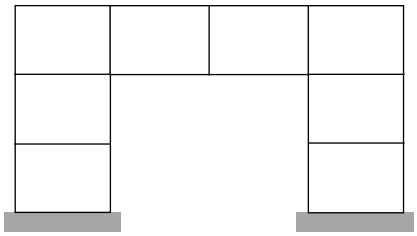

Fig. 8 Modeling of complicated shape

The benefit of macro plate model is a modeling of complicated shape shown in Fig. 8. As can be seen in Fig. 4, macro plate model can express in-plane deformation in both x- and y-directions, which was different from macroscopic models only y-direction shown in Fig. 1. As can be seen in Fig. 8, this wall was divided to eight elements of macro plate model in order to connect with beams and columns, so stiffness matrix of each element can be modified using I_x' and I_y' at the last row. In addition, the combination in the last row of stiffness matrix can express the deformation shape of a wall shown in

Fig. 6(a). Therefore, any complicated shapes of a wall can be modeled using macro plate model.

4. OUT-OF-PLANE BEHAVIOR OF MACRO PLATE MODEL

As aforementioned above, out-of-plane behavior of macro plate model was derived originally from the theory of plate bending. Out-of-plane bending and anti-symmetric out-of-plane bending deformation are expressed in term of rotational deformations about the x- and y-axes (τ_x and τ_y) shown in Fig. 9(a) and Fig. 9(b) respectively. Out-of-plane torsional deformation (ϕ_{xy}) are expressed in Fig. 9(c).

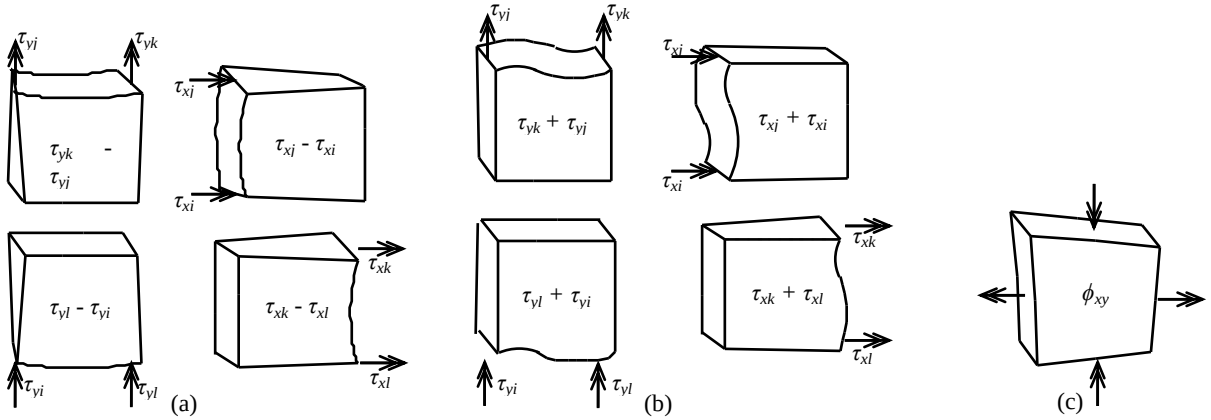

Fig. 9 (a) Out-of-plane bending deformation, (b) Anti-symmetric out-of-plane bending deformation, and (c) Out-of-plane torsional deformation

The deformation-displacement relationship of out-of-plane behavior was derived as Eq. (2).

$$\begin{bmatrix}\tau_{yi}\\ \tau_{yj}\\ \tau_{yk}\\ \tau_{yl}\\ \tau_{xi}\\ \tau_{xj}\\ \tau_{xk}\\ \tau_{xl}\\ \phi_{xy}\end{bmatrix} = \begin{bmatrix} -1/l_x & 0 & 1 & 0 & 0 & 0 & 0 & 0 & 0 & 1/l_x & 0 & 0\\ 0 & 0 & 0 & -1/l_x & 0 & 1 & 1/l_x & 0 & 0 & 0 & 0 & 0\\ 0 & 0 & 0 & -1/l_x & 0 & 0 & 1/l_x & 0 & 1 & 0 & 0 & 0\\ -1/l_x & 0 & 0 & 0 & 0 & 0 & 0 & 0 & 0 & 1/l_x & 0 & 1\\ 1/l_y & 1 & 0 & -1/l_y & 0 & 0 & 0 & 0 & 0 & 0 & 0 & 0\\ 1/l_y & 0 & 0 & -1/l_y & 1 & 0 & 0 & 0 & 0 & 0 & 0 & 0\\ 0 & 0 & 0 & 0 & 0 & 0 & -1/l_y & 1 & 0 & 1/l_y & 0 & 0\\ 0 & 0 & 0 & 0 & 0 & 0 & -1/l_y & 0 & 0 & 1/l_y & 1 & 0\\ 1/l_x l_y & 0 & 0 & -1/l_x l_y & 0 & 0 & 1/l_x l_y & 0 & 0 & -1/l_x l_y & 0 & 0 \end{bmatrix} \begin{bmatrix} w_i\\ \theta_{xi}\\ \theta_{yi}\\ w_j\\ \theta_{xj}\\ \theta_{yj}\\ w_k\\ \theta_{xk}\\ \theta_{yk}\\ w_l\\ \theta_{xl}\\ \theta_{yl}\end{bmatrix} \quad (2)$$

Theory of plate bending (Zienkiewicz et al., 2005) was conducted to derive out-of-plane stiffness matrix of macro plate model from out-of-plane shape function of plate bending as Eq. (3).

$$w_i = \alpha_1 + \alpha_2 x_i + \alpha_3 y_i + \alpha_4 x_i^2 + \alpha_5 x_i y_i + \alpha_6 y_i^2 + \alpha_7 x_i^3 + \alpha_8 x_i^2 y_i + \alpha_9 x_i y_i^2 + \alpha_{10} y_i^3 + \alpha_{11} x_i^3 y_i + \alpha_{12} x_i y_i^3 \quad (3)$$

In order to derive out-of-plane stiffness matrix of macro plate model, out-of-plane nodal forces are defined shown in Fig. 10. Based on out-of-plane shape function in Eq. (3), the out-of-plane nodal force-displacement relationship is expressed as Eq. (4) referring to a component of out-of-plane bending deformation about x-and y- axes, secondary deformation due to Poisson effect, and out-of-plane torsional deformation respectively shown in Fig. 11.

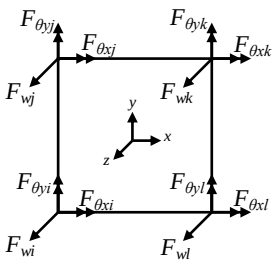

Fig. 10 Out-of-plane nodal force

$$
\begin{bmatrix} F_{w_i} \\ F_{\theta_{xi}} \\ F_{\theta_{yi}} \\ F_{w_j} \\ F_{\theta_{xj}} \\ F_{\theta_{yj}} \\ F_{w_k} \\ F_{\theta_{xk}} \\ F_{\theta_{yk}} \\ F_{w_l} \\ F_{\theta_{xl}} \\ F_{\theta_{yl}} \end{bmatrix} = EI_{zy} \begin{bmatrix} \frac{4}{l_y^3} & -\frac{2}{l_y^2} & 0 & -\frac{4}{l_y^3} & -\frac{2}{l_y^2} & 0 & -\frac{2}{l_y^3} & -\frac{1}{l_y^2} & 0 & \frac{2}{l_y^3} & -\frac{1}{l_y^2} & 0 \\ -\frac{2}{l_y^2} & \frac{4}{3l_y} & 0 & \frac{2}{l_y^2} & \frac{2}{3l_y} & 0 & \frac{1}{l_y^2} & \frac{1}{3l_y} & 0 & -\frac{1}{l_y^2} & \frac{2}{3l_y} & 0 \\ 0 & 0 & 0 & 0 & 0 & 0 & 0 & 0 & 0 & 0 & 0 & 0 \\ -\frac{4}{l_y^3} & \frac{2}{l_y^2} & 0 & \frac{4}{l_y^3} & \frac{2}{l_y^2} & 0 & \frac{2}{l_y^3} & \frac{1}{l_y^2} & 0 & -\frac{2}{l_y^3} & \frac{1}{l_y^2} & 0 \\ -\frac{2}{l_y^2} & \frac{2}{3l_y} & 0 & \frac{2}{l_y^2} & \frac{4}{3l_y} & 0 & \frac{1}{l_y^2} & \frac{2}{3l_y} & 0 & -\frac{1}{l_y^2} & \frac{1}{3l_y} & 0 \\ 0 & 0 & 0 & 0 & 0 & 0 & 0 & 0 & 0 & 0 & 0 & 0 \\ -\frac{2}{l_y^3} & \frac{1}{l_y^2} & 0 & \frac{2}{l_y^3} & \frac{1}{l_y^2} & 0 & \frac{4}{l_y^3} & \frac{2}{l_y^2} & 0 & -\frac{4}{l_y^3} & \frac{2}{l_y^2} & 0 \\ -\frac{1}{l_y^2} & \frac{1}{3l_y} & 0 & \frac{1}{l_y^2} & \frac{2}{3l_y} & 0 & \frac{2}{l_y^2} & \frac{4}{3l_y} & 0 & -\frac{2}{l_y^2} & \frac{2}{3l_y} & 0 \\ 0 & 0 & 0 & 0 & 0 & 0 & 0 & 0 & 0 & 0 & 0 & 0 \\ \frac{2}{l_y^3} & -\frac{1}{l_y^2} & 0 & -\frac{2}{l_y^3} & -\frac{1}{l_y^2} & 0 & -\frac{4}{l_y^3} & -\frac{2}{l_y^2} & 0 & \frac{4}{l_y^3} & -\frac{2}{l_y^2} & 0 \\ -\frac{1}{l_y^2} & \frac{2}{3l_y} & 0 & \frac{1}{l_y^2} & \frac{1}{3l_y} & 0 & \frac{2}{l_y^2} & \frac{2}{3l_y} & 0 & -\frac{2}{l_y^2} & \frac{4}{3l_y} & 0 \\ 0 & 0 & 0 & 0 & 0 & 0 & 0 & 0 & 0 & 0 & 0 & 0 \end{bmatrix} + EI_{zx} \begin{bmatrix} \frac{4}{l_x^3} & 0 & \frac{2}{l_x^2} & \frac{2}{l_x^3} & 0 & \frac{1}{l_x^2} & -\frac{2}{l_x^3} & 0 & \frac{1}{l_x^2} & -\frac{4}{l_x^3} & 0 & \frac{2}{l_x^2} \\ 0 & 0 & 0 & 0 & 0 & 0 & 0 & 0 & 0 & 0 & 0 & 0 \\ \frac{2}{l_x^2} & 0 & \frac{4}{3l_x} & \frac{1}{l_x^2} & 0 & \frac{2}{3l_x} & -\frac{1}{l_x^2} & 0 & \frac{1}{3l_x} & -\frac{2}{l_x^2} & 0 & \frac{2}{3l_x} \\ \frac{2}{l_x^3} & 0 & \frac{1}{l_x^2} & \frac{4}{l_x^3} & 0 & \frac{2}{l_x^2} & -\frac{4}{l_x^3} & 0 & \frac{2}{l_x^2} & -\frac{2}{l_x^3} & 0 & \frac{1}{l_x^2} \\ 0 & 0 & 0 & 0 & 0 & 0 & 0 & 0 & 0 & 0 & 0 & 0 \\ \frac{1}{l_x^2} & 0 & \frac{2}{3l_x} & \frac{2}{l_x^2} & 0 & \frac{4}{3l_x} & -\frac{2}{l_x^2} & 0 & \frac{2}{3l_x} & -\frac{1}{l_x^2} & 0 & \frac{1}{3l_x} \\ -\frac{2}{l_x^3} & 0 & -\frac{1}{l_x^2} & -\frac{4}{l_x^3} & 0 & -\frac{2}{l_x^2} & \frac{4}{l_x^3} & 0 & -\frac{2}{l_x^2} & \frac{2}{l_x^3} & 0 & -\frac{1}{l_x^2} \\ 0 & 0 & 0 & 0 & 0 & 0 & 0 & 0 & 0 & 0 & 0 & 0 \\ \frac{1}{l_x^2} & 0 & \frac{1}{3l_x} & \frac{2}{l_x^2} & 0 & \frac{2}{3l_x} & -\frac{2}{l_x^2} & 0 & \frac{4}{3l_x} & -\frac{1}{l_x^2} & 0 & \frac{2}{3l_x} \\ -\frac{4}{l_x^3} & 0 & -\frac{2}{l_x^2} & -\frac{2}{l_x^3} & 0 & -\frac{1}{l_x^2} & \frac{2}{l_x^3} & 0 & -\frac{1}{l_x^2} & \frac{4}{l_x^3} & 0 & -\frac{2}{l_x^2} \\ 0 & 0 & 0 & 0 & 0 & 0 & 0 & 0 & 0 & 0 & 0 & 0 \\ \frac{2}{l_x^2} & 0 & \frac{2}{3l_x} & \frac{1}{l_x^2} & 0 & \frac{1}{3l_x} & -\frac{1}{l_x^2} & 0 & \frac{2}{3l_x} & 0 & -\frac{2}{l_x^2} & \frac{4}{3l_x} \end{bmatrix}
$$

$$
+\frac{vEt^3}{12} \begin{bmatrix} \frac{2}{l_x l_y} & -\frac{1}{l_x} & \frac{1}{l_y} & -\frac{2}{l_x l_y} & 0 & -\frac{1}{l_y} & \frac{2}{l_x l_y} & 0 & 0 & -\frac{2}{l_x l_y} & \frac{1}{l_x} & 0 \\ \frac{1}{l_x} & 0 & -1 & 0 & 0 & 0 & 0 & 0 & 0 & \frac{1}{l_x} & 0 & 0 \\ \frac{1}{l_y} & -1 & 0 & -\frac{1}{l_y} & 0 & 0 & 0 & 0 & 0 & 0 & 0 & 0 \\ -\frac{2}{l_x l_y} & 0 & -\frac{1}{l_y} & \frac{2}{l_x l_y} & \frac{1}{l_x} & \frac{1}{l_y} & -\frac{2}{l_x l_y} & -\frac{1}{l_x} & 0 & \frac{2}{l_x l_y} & 0 & 0 \\ 0 & 0 & 0 & \frac{1}{l_x} & 0 & 1 & -\frac{1}{l_x} & 0 & 0 & 0 & 0 & 0 \\ -\frac{1}{l_y} & 0 & 0 & \frac{1}{l_y} & 1 & 0 & 0 & 0 & 0 & 0 & 0 & 0 \\ \frac{2}{l_x l_y} & 0 & 0 & -\frac{2}{l_x l_y} & -\frac{1}{l_x} & 0 & \frac{2}{l_x l_y} & \frac{1}{l_x} & -\frac{1}{l_y} & -\frac{2}{l_x l_y} & 0 & \frac{1}{l_y} \\ 0 & 0 & 0 & -\frac{1}{l_x} & 0 & 0 & \frac{1}{l_x} & 0 & -1 & 0 & 0 & 0 \\ 0 & 0 & 0 & 0 & 0 & 0 & -\frac{1}{l_y} & -1 & 0 & \frac{1}{l_y} & 0 & 0 \\ -\frac{2}{l_x l_y} & \frac{1}{l_x} & 0 & \frac{2}{l_x l_y} & 0 & 0 & -\frac{2}{l_x l_y} & 0 & \frac{1}{l_y} & \frac{2}{l_x l_y} & -\frac{1}{l_x} & -\frac{1}{l_y} \\ \frac{1}{l_x} & 0 & 0 & 0 & 0 & 0 & 0 & 0 & 0 & -\frac{1}{l_x} & 0 & 1 \\ 0 & 0 & 0 & 0 & 0 & 0 & \frac{1}{l_y} & 0 & 0 & -\frac{1}{l_y} & 1 & 0 \end{bmatrix} + \frac{Gt^3}{30} \begin{bmatrix} \frac{14}{l_x l_y} & -\frac{1}{l_x} & \frac{1}{l_y} & -\frac{14}{l_x l_y} & -\frac{1}{l_x} & -\frac{1}{l_y} & \frac{14}{l_x l_y} & \frac{1}{l_x} & -\frac{1}{l_y} & -\frac{14}{l_x l_y} & \frac{1}{l_x} & \frac{1}{l_y} \\ -\frac{1}{l_x} & \frac{4l_y}{3l_x} & 0 & \frac{1}{l_x} & -\frac{l_y}{3l_x} & 0 & -\frac{1}{l_x} & \frac{l_y}{3l_x} & 0 & \frac{1}{l_x} & -\frac{4l_y}{3l_x} & 0 \\ \frac{1}{l_y} & 0 & \frac{4l_x}{3l_y} & -\frac{1}{l_y} & 0 & -\frac{4l_x}{3l_y} & \frac{1}{l_y} & 0 & \frac{l_x}{3l_y} & -\frac{1}{l_y} & 0 & -\frac{l_x}{3l_y} \\ -\frac{14}{l_x l_y} & \frac{1}{l_x} & -\frac{1}{l_y} & \frac{14}{l_x l_y} & \frac{1}{l_x} & \frac{1}{l_y} & -\frac{14}{l_x l_y} & -\frac{1}{l_x} & \frac{1}{l_y} & \frac{14}{l_x l_y} & -\frac{1}{l_x} & -\frac{1}{l_y} \\ -\frac{1}{l_x} & -\frac{l_y}{3l_x} & 0 & \frac{1}{l_x} & \frac{4l_y}{3l_x} & 0 & -\frac{1}{l_x} & -\frac{4l_y}{3l_x} & 0 & \frac{1}{l_x} & \frac{4l_y}{3l_x} & 0 \\ -\frac{1}{l_y} & 0 & -\frac{4l_x}{3l_y} & \frac{1}{l_y} & 0 & \frac{4l_x}{3l_y} & -\frac{1}{l_y} & 0 & -\frac{l_x}{3l_y} & \frac{1}{l_y} & 0 & \frac{l_x}{3l_y} \\ \frac{14}{l_x l_y} & -\frac{1}{l_x} & \frac{1}{l_y} & -\frac{14}{l_x l_y} & -\frac{1}{l_x} & -\frac{1}{l_y} & \frac{14}{l_x l_y} & \frac{1}{l_x} & -\frac{1}{l_y} & -\frac{14}{l_x l_y} & \frac{1}{l_x} & \frac{1}{l_y} \\ \frac{1}{l_x} & \frac{l_y}{3l_x} & 0 & -\frac{1}{l_x} & -\frac{4l_y}{3l_x} & 0 & \frac{1}{l_x} & \frac{4l_y}{3l_x} & 0 & -\frac{1}{l_x} & -\frac{l_y}{3l_x} & 0 \\ -\frac{1}{l_y} & 0 & \frac{l_x}{3l_y} & \frac{1}{l_y} & 0 & -\frac{l_x}{3l_y} & -\frac{1}{l_y} & 0 & \frac{4l_x}{3l_y} & \frac{1}{l_y} & 0 & -\frac{4l_x}{3l_y} \\ -\frac{14}{l_x l_y} & \frac{1}{l_x} & -\frac{1}{l_y} & \frac{14}{l_x l_y} & \frac{1}{l_x} & \frac{1}{l_y} & -\frac{14}{l_x l_y} & -\frac{1}{l_x} & \frac{1}{l_y} & \frac{14}{l_x l_y} & -\frac{1}{l_x} & -\frac{1}{l_y} \\ \frac{1}{l_x} & -\frac{4l_y}{3l_x} & 0 & -\frac{1}{l_x} & \frac{4l_y}{3l_x} & 0 & \frac{1}{l_x} & -\frac{l_y}{3l_x} & 0 & -\frac{1}{l_x} & \frac{l_y}{3l_x} & 0 \\ \frac{1}{l_y} & 0 & -\frac{l_x}{3l_y} & -\frac{1}{l_y} & 0 & \frac{l_x}{3l_y} & \frac{1}{l_y} & 0 & -\frac{4l_x}{3l_y} & -\frac{1}{l_y} & 0 & \frac{4l_x}{3l_y} \end{bmatrix} \begin{bmatrix} w_i \\ \theta_{xi} \\ \theta_{yi} \\ w_j \\ \theta_{xj} \\ \theta_{yj} \\ w_k \\ \theta_{xk} \\ \theta_{yk} \\ w_l \\ \theta_{xl} \\ \theta_{yl} \end{bmatrix} \quad (4)
$$

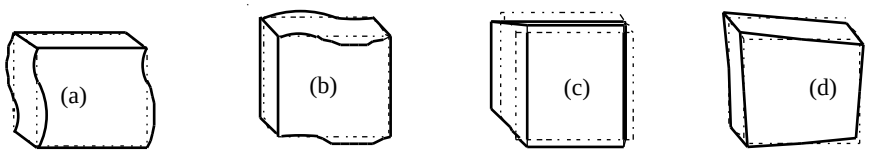

Fig. 11 (a) Out-of-plane bending deformation about x-axis, (b) bending deformation about y-axis, (c) Secondary deformation due to Poisson effect, and (d) Out-of-plane torsional deformation

Referring to modes of out-of-plane deformation in Fig. 11, the first term of Eq. (4) is a component of out-of-plane bending deformation about the x-axis shown in Fig. 11(a). The second term is a component of out-of-plane bending deformation about the y-axis shown in Fig. 11(b). The third term is a component of secondary deformation due to Poisson effect shown in Fig. 11(c). The fourth term is a component of out-of-plane torsional deformation shown in Fig. 11(d).

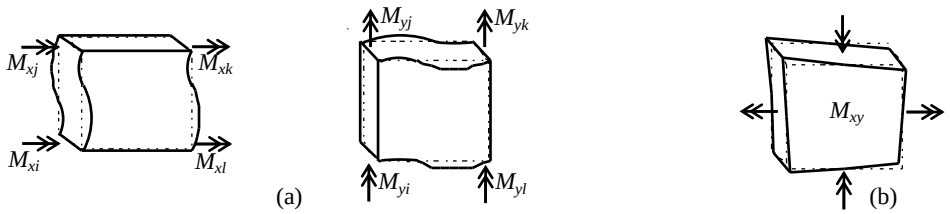

Fig. 12 (a) Out-of-plane bending moment about x- and y-axis and (b) Out-of-plane torsional moment

According to modes of out-of-plane deformation in Fig. 11, out-of-plane bending moment is

expressed in Fig. 12(a) including the effect of secondary and torsional deformation in Fig. 11(c) and Fig. 11(d) respectively. In addition, out-of-plane torsional moment is expressed in Fig. 12(b).

The decomposition of out-of-plane bending moment shown in Fig. 12(a) is expressed as Eq. (5). The first term was a component of out-of-plane pure bending moment about the x- and y-axes. The second term was a component of out-of-plane bending moment due to Poisson effect. The third term was a component of out-of-plane bending moment due to torsional effect. In addition, out-of-plane torsional moment shown in Fig. 12(b) is expressed as Eq. (6).

$$\begin{bmatrix} M_{xi} \\ M_{xj} \\ M_{xk} \\ M_{xl} \\ M_{yi} \\ M_{yj} \\ M_{yk} \\ M_{yl} \end{bmatrix} = \begin{bmatrix} M'_{xi} \\ M'_{xj} \\ M'_{xk} \\ M'_{xl} \\ M'_{yi} \\ M'_{yj} \\ M'_{yk} \\ M'_{yl} \end{bmatrix} + \begin{bmatrix} M''_{xi} \\ M''_{xj} \\ M''_{xk} \\ M''_{xl} \\ M''_{yi} \\ M''_{yj} \\ M''_{yk} \\ M''_{yl} \end{bmatrix} + \begin{bmatrix} M'''_{xi} \\ M'''_{xj} \\ M'''_{xk} \\ M'''_{xl} \\ M'''_{yi} \\ M'''_{yj} \\ M'''_{yk} \\ M'''_{yl} \end{bmatrix} \tag{5}$$

$$M_{xy} = \frac{Gt^3 l_x l_y}{3} \phi_{xy} \tag{6}$$

In order to obtain stiffness matrix of each component in Eq. (5), the nodal force-displacement relationship in Eq. (4) can be solved from Eq. (2). Referring to Fig. 11(a) and Fig. 11(b), the stiffness matrices of out-of-plane bending moment from pure deformation about the x- and y-axes respectively are expressed as Eq. (7).

$$\begin{bmatrix} M'_{xi} \\ M'_{xj} \\ M'_{xk} \\ M'_{xl} \end{bmatrix} = \frac{EI_{zy}}{3l_y} \begin{bmatrix} 4 & 2 & 1 & 2 \\ 2 & 4 & 2 & 1 \\ 1 & 2 & 4 & 2 \\ 2 & 1 & 2 & 4 \end{bmatrix} \begin{bmatrix} \tau_{xi} \\ \tau_{xj} \\ \tau_{xk} \\ \tau_{xl} \end{bmatrix} \qquad \begin{bmatrix} M'_{yi} \\ M'_{yj} \\ M'_{yk} \\ M'_{yl} \end{bmatrix} = \frac{EI_{zx}}{3l_x} \begin{bmatrix} 4 & 2 & 1 & 2 \\ 2 & 4 & 2 & 1 \\ 1 & 2 & 4 & 2 \\ 2 & 1 & 2 & 4 \end{bmatrix} \begin{bmatrix} \tau_{yi} \\ \tau_{yj} \\ \tau_{yk} \\ \tau_{yl} \end{bmatrix} \tag{7}$$

Referring to Fig. 11(c), the stiffness matrix of out-of-plane bending moment due to Poisson effect is expressed as Eq. (8).

$$\begin{bmatrix} M''_{xi} \\ M''_{xj} \\ M''_{xk} \\ M''_{xl} \\ M''_{yi} \\ M''_{yj} \\ M''_{yk} \\ M''_{yl} \end{bmatrix} = \nu E \frac{t^3}{12} \begin{bmatrix} 0 & 0 & 0 & 0 & -1 & 0 & 0 & 0 \\ 0 & 0 & 0 & 0 & 0 & 1 & 0 & 0 \\ 0 & 0 & 0 & 0 & 0 & 0 & -1 & 0 \\ 0 & 0 & 0 & 0 & 0 & 0 & 0 & 1 \\ -1 & 0 & 0 & 0 & 0 & 0 & 0 & 0 \\ 0 & 1 & 0 & 0 & 0 & 0 & 0 & 0 \\ 0 & 0 & -1 & 0 & 0 & 0 & 0 & 0 \\ 0 & 0 & 0 & 1 & 0 & 0 & 0 & 0 \end{bmatrix} \begin{bmatrix} \tau_{xi} \\ \tau_{xj} \\ \tau_{xk} \\ \tau_{xl} \\ \tau_{yi} \\ \tau_{yj} \\ \tau_{yk} \\ \tau_{yl} \end{bmatrix} \tag{8}$$

Referring to Fig. 11(d), the stiffness matrix of out-of-plane bending moment due to torsional effect is expressed as Eq. (9).

$$\begin{bmatrix} M'''_{xi} \\ M'''_{xj} \\ M'''_{xk} \\ M'''_{xl} \end{bmatrix} = \frac{Gt^3 l_x}{90 l_y} \begin{bmatrix} 4 & -1 & 1 & -4 \\ -1 & 4 & -4 & 1 \\ 1 & -4 & 4 & -1 \\ -4 & 1 & -1 & 4 \end{bmatrix} \begin{bmatrix} \tau_{xi} \\ \tau_{xj} \\ \tau_{xk} \\ \tau_{xl} \end{bmatrix} \qquad \begin{bmatrix} M'''_{yi} \\ M'''_{yj} \\ M'''_{yk} \\ M'''_{yl} \end{bmatrix} = \frac{Gt^3 l_y}{90 l_x} \begin{bmatrix} 4 & -4 & 1 & -1 \\ -4 & 4 & -1 & 1 \\ 1 & -1 & 4 & -4 \\ -1 & 1 & -4 & 4 \end{bmatrix} \begin{bmatrix} \tau_{yi} \\ \tau_{yj} \\ \tau_{yk} \\ \tau_{yl} \end{bmatrix} \tag{9}$$

For out-of-plane deformation, it is necessary to incorporate out-of-plane pure bending deformation in Fig. 13(a) with out-of-plane shear deformations in Fig. 13(b) in order to obtain more realistic behavior, in which out-of-plane behavior of a wall member should be more softening.

Fig. 13 (a) Out-of-plane pure bending deformation and (b) Out-of-plane shear deformation

Using flexibility matrix, out-of-plane pure bending deformation in Fig. 13(a) was incorporated with out-of-plane shear deformation in Fig. 13(b). The flexibility matrix due to out-of-plane pure bending deformation is expressed as Eq. (10).

$$\begin{bmatrix}\tau_{xi}\\ \tau_{xj}\\ \tau_{xk}\\ \tau_{xl}\end{bmatrix}=\frac{l_y}{3EI_{zy}}\begin{bmatrix}4 & -2 & 1 & -2\\ -2 & 4 & -2 & 1\\ 1 & -2 & 4 & -2\\ -2 & 1 & -2 & 4\end{bmatrix}\begin{bmatrix}M'_{xi}\\ M'_{xj}\\ M'_{xk}\\ M'_{xl}\end{bmatrix} \qquad \begin{bmatrix}\tau_{yi}\\ \tau_{yj}\\ \tau_{yk}\\ \tau_{yl}\end{bmatrix}=\frac{l_x}{3EI_{zx}}\begin{bmatrix}4 & -2 & 1 & -2\\ -2 & 4 & -2 & 1\\ 1 & -2 & 4 & -2\\ -2 & 1 & -2 & 4\end{bmatrix}\begin{bmatrix}M'_{yi}\\ M'_{yj}\\ M'_{yk}\\ M'_{yl}\end{bmatrix} \tag{10}$$

Incorporating out-of-plane bending deformation with out-of-plane shear deformation ($\kappa M / Gtl_xl_y$), the flexibility matrix is expressed as Eq. (11).

$$\begin{bmatrix}\tau_{xi}\\ \tau_{xj}\\ \tau_{xk}\\ \tau_{xl}\end{bmatrix}=\begin{bmatrix}\frac{4l_y}{3E_{y1}I_{zy}}+\frac{\kappa_x}{G_{y1}tl_xl_y} & -\frac{2l_y}{3E_{y1}I_{zy}}+\frac{\kappa_x}{G_{y1}tl_xl_y} & \frac{l_y}{3E_{y2}I_{zy}}+\frac{\kappa_x}{G_{y2}tl_xl_y} & -\frac{2l_y}{3E_{y2}I_{zy}}+\frac{\kappa_x}{G_{y2}tl_xl_y}\\ -\frac{2l_y}{3E_{y1}I_{zy}}+\frac{\kappa_x}{G_{y1}tl_xl_y} & \frac{4l_y}{3E_{y1}I_{zy}}+\frac{\kappa_x}{G_{y1}tl_xl_y} & -\frac{2l_y}{3E_{y2}I_{zy}}+\frac{\kappa_x}{G_{y2}tl_xl_y} & \frac{l_y}{3E_{y2}I_{zy}}+\frac{\kappa_x}{G_{y2}tl_xl_y}\\ \frac{l_y}{3E_{y1}I_{zy}}+\frac{\kappa_x}{G_{y1}tl_xl_y} & -\frac{2l_y}{3E_{y1}I_{zy}}+\frac{\kappa_x}{G_{y1}tl_xl_y} & \frac{4l_y}{3E_{y2}I_{zy}}+\frac{\kappa_x}{G_{y2}tl_xl_y} & -\frac{2l_y}{3E_{y2}I_{zy}}+\frac{\kappa_x}{G_{y2}tl_xl_y}\\ -\frac{2l_y}{3E_{y1}I_{zy}}+\frac{\kappa_x}{G_{y1}tl_xl_y} & \frac{l_y}{3E_{y1}I_{zy}}+\frac{\kappa_x}{G_{y1}tl_xl_y} & -\frac{2l_y}{3E_{y2}I_{zy}}+\frac{\kappa_x}{G_{y2}tl_xl_y} & \frac{4l_y}{3E_{y2}I_{zy}}+\frac{\kappa_x}{G_{y2}tl_xl_y}\end{bmatrix}\begin{bmatrix}M'_{xi}\\ M'_{xj}\\ M'_{xk}\\ M'_{xl}\end{bmatrix} \tag{11}$$

$$\begin{bmatrix}\tau_{yi}\\ \tau_{yj}\\ \tau_{yk}\\ \tau_{yl}\end{bmatrix}=\begin{bmatrix}\frac{4l_x}{3E_{x1}I_{zx}}+\frac{\kappa_y}{G_{x1}tl_xl_y} & -\frac{2l_x}{3E_{x2}I_{zx}}+\frac{\kappa_y}{G_{x2}tl_xl_y} & \frac{l_x}{3E_{x2}I_{zx}}+\frac{\kappa_y}{G_{x2}tl_xl_y} & -\frac{2l_x}{3E_{x1}I_{zx}}+\frac{\kappa_y}{G_{x1}tl_xl_y}\\ -\frac{2l_x}{3E_{x1}I_{zx}}+\frac{\kappa_y}{G_{x1}tl_xl_y} & \frac{4l_x}{3E_{x2}I_{zx}}+\frac{\kappa_y}{G_{x2}tl_xl_y} & -\frac{2l_x}{3E_{x2}I_{zx}}+\frac{\kappa_y}{G_{x2}tl_xl_y} & \frac{l_x}{3E_{x1}I_{zx}}+\frac{\kappa_y}{G_{x1}tl_xl_y}\\ \frac{l_x}{3E_{x1}I_{zx}}+\frac{\kappa_y}{G_{x1}tl_xl_y} & -\frac{2l_x}{3E_{x2}I_{zx}}+\frac{\kappa_y}{G_{x2}tl_xl_y} & \frac{4l_x}{3E_{x2}I_{zx}}+\frac{\kappa_y}{G_{x2}tl_xl_y} & -\frac{2l_x}{3E_{x1}I_{zx}}+\frac{\kappa_y}{G_{x1}tl_xl_y}\\ -\frac{2l_x}{3E_{x1}I_{zx}}+\frac{\kappa_y}{G_{x1}tl_xl_y} & \frac{l_x}{3E_{x2}I_{zx}}+\frac{\kappa_y}{G_{x2}tl_xl_y} & -\frac{2l_x}{3E_{x2}I_{zx}}+\frac{\kappa_y}{G_{x2}tl_xl_y} & \frac{4l_x}{3E_{x1}I_{zx}}+\frac{\kappa_y}{G_{x1}tl_xl_y}\end{bmatrix}\begin{bmatrix}M'_{yi}\\ M'_{yj}\\ M'_{yk}\\ M'_{yl}\end{bmatrix}$$

From the flexibility matrix in Eq. (11), the stiffness matrix of out-of-plane pure bending deformation incorporating with out-of-plane shear deformation is expressed as Eq. (12).

$$\begin{bmatrix}M'_{xi}\\ M'_{xj}\\ M'_{xk}\\ M'_{xl}\end{bmatrix}=\begin{bmatrix}\frac{8+2\lambda_{y1}+5\lambda_{y2}}{6(1+\lambda_{y1}+\lambda_{y2})}\frac{E_{y1}I_{zy}}{l_y} & \frac{4-2\lambda_{y1}+\lambda_{y2}}{6(1+\lambda_{y1}+\lambda_{y2})}\frac{E_{y1}I_{zy}}{l_y} & \frac{2-\lambda_{y1}-4\lambda_{y2}}{6(1+\lambda_{y1}+\lambda_{y2})}\frac{E_{y1}I_{zy}}{l_y} & \frac{4+\lambda_{y1}-2\lambda_{y2}}{6(1+\lambda_{y1}+\lambda_{y2})}\frac{E_{y1}I_{zy}}{l_y}\\ \frac{4-2\lambda_{y1}+\lambda_{y2}}{6(1+\lambda_{y1}+\lambda_{y2})}\frac{E_{y1}I_{zy}}{l_y} & \frac{8+2\lambda_{y1}+5\lambda_{y2}}{6(1+\lambda_{y1}+\lambda_{y2})}\frac{E_{y1}I_{zy}}{l_y} & \frac{4+\lambda_{y1}-2\lambda_{y2}}{6(1+\lambda_{y1}+\lambda_{y2})}\frac{E_{y1}I_{zy}}{l_y} & \frac{2-\lambda_{y1}-4\lambda_{y2}}{6(1+\lambda_{y1}+\lambda_{y2})}\frac{E_{y1}I_{zy}}{l_y}\\ \frac{2-4\lambda_{y1}-\lambda_{y2}}{6(1+\lambda_{y1}+\lambda_{y2})}\frac{E_{y2}I_{zy}}{l_y} & \frac{4-2\lambda_{y1}+\lambda_{y2}}{6(1+\lambda_{y1}+\lambda_{y2})}\frac{E_{y2}I_{zy}}{l_y} & \frac{8+5\lambda_{y1}+2\lambda_{y2}}{6(1+\lambda_{y1}+\lambda_{y2})}\frac{E_{y2}I_{zy}}{l_y} & \frac{4+\lambda_{y1}-2\lambda_{y2}}{6(1+\lambda_{y1}+\lambda_{y2})}\frac{E_{y2}I_{zy}}{l_y}\\ \frac{4-2\lambda_{y1}+\lambda_{y2}}{6(1+\lambda_{y1}+\lambda_{y2})}\frac{E_{y2}I_{zy}}{l_y} & \frac{2-4\lambda_{y1}-\lambda_{y2}}{6(1+\lambda_{y1}+\lambda_{y2})}\frac{E_{y2}I_{zy}}{l_y} & \frac{4+\lambda_{y1}-2\lambda_{y2}}{6(1+\lambda_{y1}+\lambda_{y2})}\frac{E_{y2}I_{zy}}{l_y} & \frac{8+5\lambda_{y1}+2\lambda_{y2}}{6(1+\lambda_{y1}+\lambda_{y2})}\frac{E_{y2}I_{zy}}{l_y}\end{bmatrix}\begin{bmatrix}\tau_{xi}\\ \tau_{xj}\\ \tau_{xk}\\ \tau_{xl}\end{bmatrix} \tag{12}$$

$$\begin{bmatrix}M'_{yi}\\ M'_{yj}\\ M'_{yk}\\ M'_{yl}\end{bmatrix}=\begin{bmatrix}\frac{8+2\lambda_{x1}+5\lambda_{x2}}{6(1+\lambda_{x1}+\lambda_{x2})}\frac{E_{x1}I_{zx}}{l_x} & \frac{4+\lambda_{x1}-2\lambda_{x2}}{6(1+\lambda_{x1}+\lambda_{x2})}\frac{E_{x1}I_{zx}}{l_x} & \frac{2-\lambda_{x1}-4\lambda_{x2}}{6(1+\lambda_{x1}+\lambda_{x2})}\frac{E_{x1}I_{zx}}{l_x} & \frac{4-2\lambda_{x1}+\lambda_{x2}}{6(1+\lambda_{x1}+\lambda_{x2})}\frac{E_{x1}I_{zx}}{l_x}\\ \frac{4-2\lambda_{x1}+\lambda_{x2}}{6(1+\lambda_{x1}+\lambda_{x2})}\frac{E_{x2}I_{zx}}{l_x} & \frac{8+5\lambda_{x1}+2\lambda_{x2}}{6(1+\lambda_{x1}+\lambda_{x2})}\frac{E_{x2}I_{zx}}{l_x} & \frac{4+\lambda_{x1}-2\lambda_{x2}}{6(1+\lambda_{x1}+\lambda_{x2})}\frac{E_{x2}I_{zx}}{l_x} & \frac{2-4\lambda_{x1}-\lambda_{x2}}{6(1+\lambda_{x1}+\lambda_{x2})}\frac{E_{x2}I_{zx}}{l_x}\\ \frac{2-4\lambda_{x1}-\lambda_{x2}}{6(1+\lambda_{x1}+\lambda_{x2})}\frac{E_{x2}I_{zx}}{l_x} & \frac{4+\lambda_{x1}-2\lambda_{x2}}{6(1+\lambda_{x1}+\lambda_{x2})}\frac{E_{x2}I_{zx}}{l_x} & \frac{8+5\lambda_{x1}+2\lambda_{x2}}{6(1+\lambda_{x1}+\lambda_{x2})}\frac{E_{x2}I_{zx}}{l_x} & \frac{4-2\lambda_{x1}+\lambda_{x2}}{6(1+\lambda_{x1}+\lambda_{x2})}\frac{E_{x2}I_{zx}}{l_x}\\ \frac{4-2\lambda_{x1}+\lambda_{x2}}{6(1+\lambda_{x1}+\lambda_{x2})}\frac{E_{x1}I_{zx}}{l_x} & \frac{2-\lambda_{x1}-4\lambda_{x2}}{6(1+\lambda_{x1}+\lambda_{x2})}\frac{E_{x1}I_{zx}}{l_x} & \frac{4+\lambda_{x1}-2\lambda_{x2}}{6(1+\lambda_{x1}+\lambda_{x2})}\frac{E_{x1}I_{zx}}{l_x} & \frac{8+2\lambda_{x1}+5\lambda_{x2}}{6(1+\lambda_{x1}+\lambda_{x2})}\frac{E_{x1}I_{zx}}{l_x}\end{bmatrix}\begin{bmatrix}\tau_{yi}\\ \tau_{yj}\\ \tau_{yk}\\ \tau_{yl}\end{bmatrix}$$

$$\lambda_{x1}=\frac{6E_{x1}I_{zx}\kappa_y}{G_{x1}tl_x^2l_y} \qquad \lambda_{x2}=\frac{6E_{x2}I_{zx}\kappa_y}{G_{x2}tl_x^2l_y} \qquad \lambda_{y1}=\frac{6E_{y1}I_{zy}\kappa_x}{G_{y1}tl_xl_y^2} \qquad \lambda_{y2}=\frac{6E_{y2}I_{zy}\kappa_x}{G_{y2}tl_xl_y^2}$$

5. EQUILIBRIUM CONDITION OF MACRO PLATE MODEL

From aforementioned derivation, it is necessary to satisfy member force of macro plate model in Fig. 5 with equilibrium condition in Fig. 14(b).

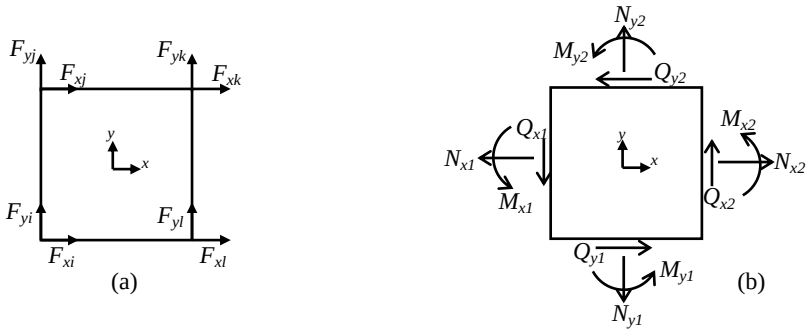

Fig. 14 (a) In-plane nodal force and (b) Member forces in equilibrium condition

From Fig. 14(a) and Fig. 5, the nodal force-member force relationship is expressed as Eq. (13) using the transpose matrix in Eq. (1).

$$\begin{bmatrix}F_{xi}\\F_{yi}\\F_{xj}\\F_{yj}\\F_{xk}\\F_{yk}\\F_{xl}\\F_{yl}\end{bmatrix}=\begin{bmatrix}-1/2 & 0 & -1/l_y & 0 & 1/2l_y\\ 0 & -1/2 & 0 & 1/l_x & 1/2l_x\\ -1/2 & 0 & 1/l_y & 0 & -1/2l_y\\ 0 & 1/2 & 0 & -1/l_x & 1/2l_x\\ 1/2 & 0 & -1/l_y & 0 & -1/2l_y\\ 0 & 1/2 & 0 & 1/l_x & -1/2l_x\\ 1/2 & 0 & 1/l_y & 0 & 1/2l_y\\ 0 & -1/2 & 0 & -1/l_x & -1/2l_x\end{bmatrix}\begin{bmatrix}N_x\\N_y\\M_x\\M_y\\M_0\end{bmatrix} \tag{13}$$

As shown in Fig. 14, member force in equilibrium condition can be converted to in-plane nodal force. With the relationship in Eq. (13), member force in equilibrium condition is expressed as Eq. (14).

$$M_{x1}=\frac{l_y}{2}(F_{xi}-F_{xj})=\frac{l_y}{2}\left(-\frac{N_x}{2}-\frac{M_x}{l_y}+\frac{M_0}{2l_y}+\frac{N_x}{2}-\frac{M_x}{l_y}+\frac{M_0}{2l_y}\right)=-M_x+\frac{M_0}{2} \tag{14}$$

$$N_{x1}=-F_{xi}-F_{xj}=\frac{N_x}{2}+\frac{M_x}{l_y}-\frac{M_0}{2l_y}+\frac{N_x}{2}-\frac{M_x}{l_y}+\frac{M_0}{2l_y}=N_x$$

$$Q_{x1}=-F_{yi}-F_{yj}==-M_0/l_x$$

Other member forces in equilibrium condition are expressed as Eq. (15).

$$M_{x2}=M_x+\frac{M_0}{2},\ N_{x2}=N_x,\ Q_{x2}=-\frac{M_0}{l_x},\ M_{y1}=-M_y-\frac{M_0}{2},\ N_{y1}=N_y,\ Q_{y1}=\frac{M_0}{l_y},\ M_{y2}=M_y-\frac{M_0}{2},\ N_{y2}=N_y,Q_{y2}=\frac{M_0}{l_y} \tag{15}$$

Therefore, equilibrium condition of axial forces was satisfied as Eq. (16)

$$N_{x1}=N_{x2}=N_x \qquad N_{y1}=N_{y2}=N_y \tag{16}$$

Also, equilibrium condition of bending moments was satisfied as Eq. (17)

$$\frac{M_{x2}-M_{x1}}{2}=\frac{M_x+\frac{M_0}{2}+M_x-\frac{M_0}{2}}{2}=M_x \qquad \frac{M_{y2}-M_{y1}}{2}=\frac{M_y+\frac{M_0}{2}+M_y-\frac{M_0}{2}}{2}=M_y \tag{17}$$

For in-plane shear deformation, shear forces can be determined from bending moments as Eq. (18). Then, shear stresses in Eq. (19) are equal to satisfy equilibrium condition.

$$Q_x=\frac{M_{x1}+M_{x2}}{l_x}=\frac{-M_x+\frac{M_0}{2}+M_x+\frac{M_0}{2}}{l_x}=\frac{M_0}{l_x} \qquad Q_y=\frac{-M_{y1}-M_{y2}}{l_y}=\frac{M_y+\frac{M_0}{2}-M_y+\frac{M_0}{2}}{l_y}=\frac{M_0}{l_y} \tag{18}$$

$$q_{xy}=\frac{Q_x}{A_{sx}}=\frac{\kappa M_0}{tl_xl_y} \qquad q_{yx}=\frac{Q_y}{A_{sy}}=\frac{\kappa M_0}{tl_yl_x} \tag{19}$$

6. DERIVATION OF STRESS AND STRAIN FOR HYSTERETIC RULES

For nonlinear analysis of RC walls represented MVLEM and IPEM, hysteretic behavior of a wall member have been described using hysteretic constitutive models of steel and concrete. As same as TVLEM, hysteretic behavior of macro plate model can be simulated in the level of a wall member in order to predict inelastic response of the entire RC wall. For macro plate model, hysteretic behavior of a wall member was described by conventional hysteretic rules, such as Takeda model in Fig. 15(a), peak-oriented model, origin-oriented model, and axial-stiffness model (Kabeyasawa et al., 1983) in Fig. 15(b), and other hysteretic models from experimental results in order to track inelastic responses. Therefore, numerical derivation of stress and strain in macro plate model is necessary for application of hysteretic models, in which the cracking, yielding, and ultimate strength of back-bone curves in Fig. 15(c) were determined using empirical equations recommended by building design standards. For nonlinear analysis of macro plate model, nodal displacements in Fig. 3 were obtained to calculate member deformations in Fig. 4 and Fig. 9. Then, member deformations were converted to member strain in order to track a hysteretic model and return the stiffness degrading factor to next analysis step. This was an iteration method for solving nonlinear problem in macro plate model.

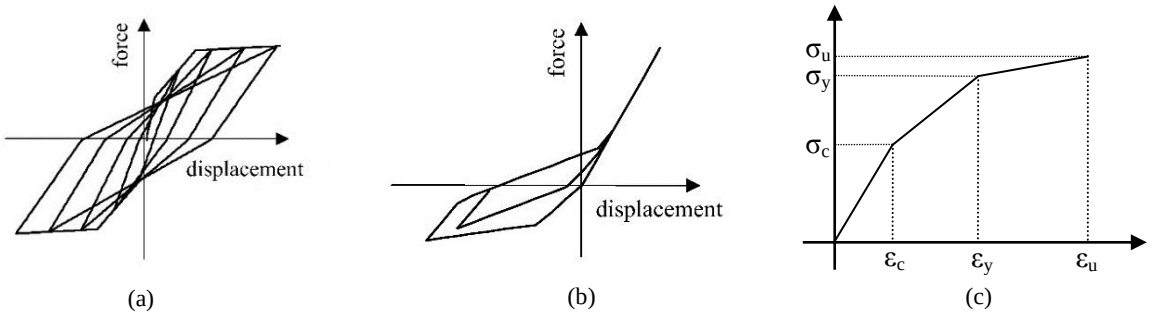

(a) (b) (c)

Fig. 15 (a) Takeda model, (b) Axial-stiffness model, and (c) Back-bone curve

6.1 In-plane behavior

Axial stress and strain of macro plate model can be derived based on the theory of elasticity ($N_x = EA_x\varepsilon_x$, $N_y = EA_y\varepsilon_y$) and the relationship in Eq. (1). The axial stress-strain relationships of macro plate model are expressed as Eq. (20).

$$N_x=\frac{1}{1-\nu^2}\left[\frac{EA_x}{l_x}\delta_x+\nu\frac{EA_x}{l_y}\delta_y\right],\ \varepsilon_x=\frac{1}{1-\nu^2}\left[\frac{\delta_x}{l_x}+\nu\frac{\delta_y}{l_y}\right] \qquad N_y=\frac{1}{1-\nu^2}\left[\nu\frac{EA_y}{l_x}\delta_x+\frac{EA_y}{l_y}\delta_y\right],\ \varepsilon_y=\frac{1}{1-\nu^2}\left[\frac{\delta_y}{l_y}+\nu\frac{\delta_x}{l_x}\right] \tag{20}$$

In-plane bending moment and curvature of macro plate model can be derived based on the theory of elasticity ($M_x = EI_x\phi_x$, $M_y = EI_y\phi_y$) and the relationship in Eq. (1). The bending moment-curvature relationships of macro plate model are expressed as Eq. (21).

$$M_x = \frac{EI_x}{l_x}\tau_x,\ \phi_x = \frac{\tau_x}{l_x} \qquad M_y = \frac{EI_y}{l_y}\tau_y,\ \phi_y = \frac{\tau_y}{l_y} \tag{21}$$

In-plane shear stress and strain of macro plate model can be derived based on the theory of elasticity ($M_0 = Gtl_xl_y\gamma_{xy} / \kappa$) and the relationship in Eq. (1). The shear stress-strain relationship of macro plate model is expressed as Eq. (22).

$$M_0 = \frac{\tau_0}{\frac{\kappa}{Gtl_xl_y} + \frac{l_x}{12EI_x'} + \frac{l_y}{12EI_y'}},\ \gamma_{xy} = \frac{\tau_0}{\frac{Gtl_x^2l_y}{12EI_x'\kappa} + \frac{Gtl_xl_y^2}{12EI_y'\kappa} + 1} \tag{22}$$

In order to propose nonlinear analysis of macro plate model for in-plane behavior, a nonlinear analytical model assembled by macro plate model of shear walls was compared with a full-scale shaking table test on a six-story RC wall-frame building carried out at E-Defense in 2006 and TVLEM (Kim et al., 2008). Three ground motion components in the east-west, north-south, and up-down direction of Kobe earthquake recorded by Japan Meteorological Agency (JMA 1995) were an input ground motion as same as the test at E-Defense. In order to neglect strength degradation in post-peak response, 25% and 50% of input ground motion were applied to verify macro plate model. For nonlinear analysis of macro plate model in this verification, Takeda model in Fig. 15(a) was applied to simulate in-plane flexural and shear behavior and axial-stiffness model in Fig. 15(b) was applied to simulate axial behavior. The back-bone curves of a wall member were determined using empirical equations recommended by AIJ standards. From analysis and experimental results, the relationship between base shear and relative displacement at 2nd floor in x- and y-directions was considered for this verification. The verification results of macro plate model (MPM) in Fig. 16 show a good correlation with the TVLEM results and the experimental results at E-Defense for 25% and 50% of input ground motion.

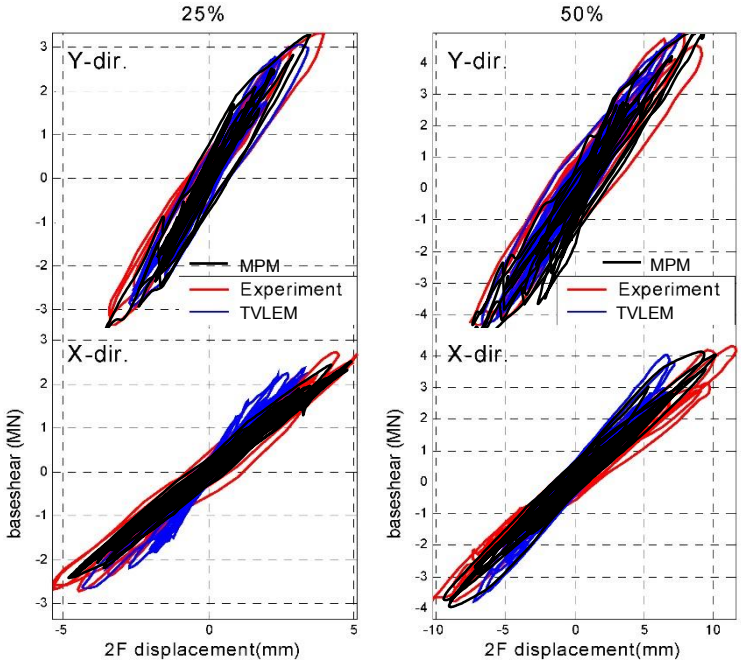

Fig. 16 Verification results of macro plate model (MPM)

6.2 Out-of-plane behavior

Out-of-plane curvature occurring in a wall member is varied depending on location. For the same nonlinear behavior as in-plane bending, member-end moments are averaged to determine curvature shown in Fig. 17. Average moment and shear force can be evaluated from member-end moments shown in Eq. (23).

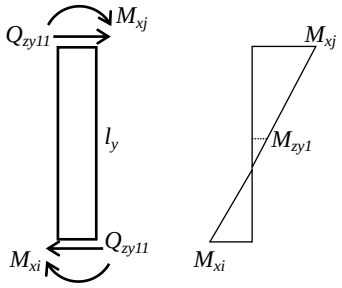

Fig. 17 Average moment

$$\begin{bmatrix} M_{zy1} \\ Q_{zy1} \\ M_{zy2} \\ Q_{zy2} \end{bmatrix} = \begin{bmatrix} -1/2 & 1/2 & 0 & 0 \\ 1/l_y & 1/l_y & 0 & 0 \\ 0 & 0 & 1/2 & -1/2 \\ 0 & 0 & 1/l_y & 1/l_y \end{bmatrix} \begin{bmatrix} M_{xi} \\ M_{xj} \\ M_{xk} \\ M_{xl} \end{bmatrix} \tag{23}$$

Out-of-plane bending moment and curvature of macro plate model can be derived based on the theory of elasticity ($M_{zy1} = E_{y1}I_{zy}\phi_{zy1} / 2$) and the relationship of pure bending deformation in Eq. (7). The bending moment-curvature relationships of macro plate model are expressed as Eq. (24).

$$M_{zy1} = -\frac{E_{y1}I_{zy}}{3l_y}\tau_{xi} + \frac{E_{y1}I_{zy}}{3l_y}\tau_{xj} + \frac{E_{y1}I_{zy}}{6l_y}\tau_{xk} - \frac{E_{y1}I_{zy}}{6l_y}\tau_{xl},\ \phi_{zy1} = \frac{1}{3l_y}(-2\tau_{xi} + 2\tau_{xj} + \tau_{xk} - \tau_{xl}) \tag{24}$$

Out-of-plane shear stress and strain of macro plate model can be derived based on the theory of elasticity ($Q_{zy1} = G_{y1}tl_x\gamma_{zy1} / 2\kappa_x$) and the relationship of bending deformation incorporating with shear deformation in Eq. (12). The shear stress-strain relationship of macro plate model is expressed as Eq. (25).

$$\begin{aligned} Q_{zy1} &= \frac{M_{xi}}{l_y} + \frac{M_{xj}}{l_y} = \frac{E_{y1}I_{zy}}{l_y^2}\left[\frac{2+\lambda_{y2}}{1+\lambda_{y1}+\lambda_{y2}}(\tau_{xi}+\tau_{xj}) + \frac{1-\lambda_{y2}}{1+\lambda_{y1}+\lambda_{y2}}(\tau_{xk}+\tau_{xl})\right] \\ \gamma_{zy1} &= \frac{\lambda_{y1}}{3(1+\lambda_{y1}+\lambda_{y2})}\left[(2+\lambda_{y2})(\tau_{xi}+\tau_{xj}) + (1-\lambda_{y2})(\tau_{xk}+\tau_{xl})\right] \end{aligned} \tag{25}$$

7. PROBLEM OF DISTRIBUTED FORCE IN MACRO PLATE MODEL

In order to simulate out-of-plane behavior in nonlinear analysis, the stress-strain relationship of macro plate model was derived by out-of-plane deformation. Since out-of-plane behavior was derived starting from the nodal force-displacement relationship and the deformation-displacement relationship, it is necessary to convert distributed force in case of wind and tsunami to nodal force for nonlinear analysis. The shape function (N) for each node is expressed in terms of normalized coordinates (ξ and η) as Eq. (26) (Zienkiewicz et al., 2005).

$$N_a = \frac{1}{4}(1+\xi_a\xi)(1+\eta_a\eta) \qquad a = i,j,k,l \tag{26}$$

For normalized coordinates:

$$(\xi_i,\eta_i) = (-1,-1) \qquad (\xi_j,\eta_j) = (-1,1) \qquad (\xi_k,\eta_k) = (1,1) \qquad (\xi_l,\eta_l) = (1,-1)$$

The general form of distributed force (q), such as wind and tsunami, is expressed in Fig. 18.

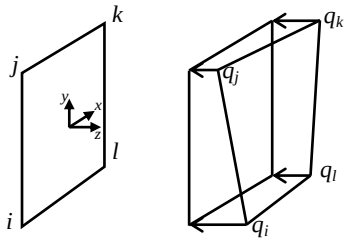

Fig. 18 Distributed force

From the shape function in Eq. (26), nodal forces acting on each node of macro plate model can be computed from Eq. (27).

$$\begin{bmatrix} F_{w_a} \\ F_{\theta_{xa}} \\ F_{\theta_{ya}} \end{bmatrix} = \frac{l_x l_y}{4} \sum_{b=i}^{k} \int_{-1}^{1} \int_{-1}^{1} \begin{bmatrix} N_a N_b q_b \\ \frac{l_y}{4} N_a N_b q_b (\eta_a - \eta) \\ \frac{l_x}{4} N_a N_b q_b (\xi_a - \xi) \end{bmatrix} d\xi d\eta \tag{27}$$

From Eq. (27), distributed force can be converted to nodal forces shown in Eq. (28).

$$\begin{bmatrix} F_{w_i} \\ F_{\theta_{xi}} \\ F_{\theta_{yi}} \end{bmatrix} = \frac{l_x l_y}{36} \begin{bmatrix} 4q_i + 2q_j + q_k + 2q_l \\ \frac{l_y}{4}(2q_i + 2q_j + q_k + q_l) \\ -\frac{l_x}{4}(2q_i + q_j + q_k + 2q_l) \end{bmatrix} \quad \begin{bmatrix} F_{w_j} \\ F_{\theta_{xj}} \\ F_{\theta_{yj}} \end{bmatrix} = \frac{l_x l_y}{36} \begin{bmatrix} 2q_i + 4q_j + 2q_k + q_l \\ -\frac{l_y}{4}(2q_i + 2q_j + q_k + q_l) \\ -\frac{l_x}{4}(q_i + 2q_j + 2q_k + q_l) \end{bmatrix}$$

$$\begin{bmatrix} F_{w_k} \\ F_{\theta_{xk}} \\ F_{\theta_{yk}} \end{bmatrix} = \frac{l_x l_y}{36} \begin{bmatrix} q_i + 2q_j + 4q_k + 2q_l \\ -\frac{l_y}{4}(q_i + q_j + 2q_k + 2q_l) \\ \frac{l_x}{4}(q_i + 2q_j + 2q_k + q_l) \end{bmatrix} \quad \begin{bmatrix} F_{w_l} \\ F_{\theta_{xl}} \\ F_{\theta_{yl}} \end{bmatrix} = \frac{l_x l_y}{36} \begin{bmatrix} 2q_i + q_j + 2q_k + 4q_l \\ \frac{l_y}{4}(q_i + q_j + 2q_k + 2q_l) \\ \frac{l_x}{4}(2q_i + q_j + q_k + 2q_l) \end{bmatrix} \tag{28}$$

8. CONCLUSIONS

For modeling of RC walls, macro plate model was proposed to describe in-plane and out-of-plane behavior of a wall member. Based on theory of elasticity and theory of plate bending, numerical derivations of macro plate model are presented in this paper. Out-of-plane bending deformation was incorporated with out-of-plane shear deformation for more softening of out-of-plane behavior. In order to predict inelastic response of a wall member, hysteretic behavior of macro plate model can be simulated by stress-strain relationships in hysteretic models. From the verification results, the analysis results show a good correlation with the TVLEM results and the experimental results at E-Defense, so macro plate model is adequate to represent shear walls for in-plane behavior. Comparing with TVLEM, MVLEM, and IPEM, macro plate model can represent any complicates shape of a wall and also can simulate out-of-plane behavior. However, strength degradation in post-peak behavior and interactions between axial, bending, and shear deformation as IPEM will be studied further.

Implementation of macro plate model, a practical model, into a computational platform will provide structural design engineers and researchers improved analytical capabilities to model and study nonlinear behavior of RC walls and their interaction with other structural members. The practical model can be used for nonlinear structural analysis of RC buildings represented by a wall-frame model. The reliability of a wall-frame model depends on hysteretic models of structural members and member interaction. This practical model allows for possible further model improvements including applications to other structural members. For out-of-plane behavior, verification and calibration using observe damage will be presented in a future publication. Moreover, nonlinear structural analysis of a wall-frame model from earthquake and subsequent tsunami, in which distributed force can be converted to nodal forces presented in this paper, will be studied further.

REFERENCES

1) Chen, S. and Kabeyasawa, T. (2000). "Modeling of RC shear wall for nonlinear analysis." *Proc., 12th World Conference on Earthquake Engineering*.
2) Chen, S., Matsumori T. and Kabeyasawa, T. (2006). "Analytical research of full-scale reinforced concrete structure test on E-Defense." *Proc., 8th U.S. National Conference on Earthquake Engineering*, No. 666.
3) Kabeyasawa, T., Shiohara, H., Otani, S. and Aoyama, H. (1983). "Analysis of the full-scale

seven-story reinforced concrete test structure." *Journal (B)*, University of Tokyo, Vol.XXXVII, 432-478.
4) Kai, Y. (2001). "A study of RC space shear wall structure for nonlinear Analysis (in Japanese)." *Doctoral Dissertation*, University of Tokyo.
5) Kim, Y., Kabeyasawa, T., Matsumori, T. and Kabeyasawa, T. (2007). "Dynamic collapse analysis of the six-story full-scale wall-frame building." *Journal of Structural Engineering Research Frontiers*.
6) Kim, Y., Kabeyasawa, T., Matsumori, T. and Kabeyasawa, T. (2008). "Analytical studies on a 6-story full-scale reinforced concrete wall-frame structure to collapse." *Proc., 14th World Conference on Earthquake Engineering*.
7) Kim, Y., Kabeyasawa, T., Matsumori, T. and Kabeyasawa, T. (2009). "Analytical study on collapse process of a full-scale 6-story reinforced concrete wall frame structure tested at E-Defense (in Japanese)." *Journal of Structural and Construction Engineering*, AIJ, Vol. 74, No. 641, 1327-1334.
8) Kim, Y., Kabeyasawa, T., Matsumori, T. and Kabeyasawa, T. (2012). "Numerical study of a full-scale six-story reinforced concrete wall-frame structure tested at E-Defense." *Journal of International Association for Earthquake Engineering*, Earthquake Engineering and Structural Dynamics, Wiley, No. 41, 1217-1239.
9) Kolozvari K. I. and Wallace J. W. (2012). "Modeling of cyclic shear–flexure interaction in reinforced concrete structural walls." *Proc., 15th World Conference on Earthquake Engineering*, No.2471.
10) Matsui, T., Kabeyasawa, T., Koto, A., Kuramoto, H. and Nagashima, I. (2004) "Shaking table test and analysis of reinforced concrete walls." *Proc., 13th World Conference on Earthquake Engineering*, No.419.
11) Milev, J. I. (1996). "Two dimensional analytical model of reinforced concrete shear walls." *Proc., 11th World Conference on Earthquake Engineering*, No.320.
12) Okamura, H. and Maekawa, K. (1991). "Nonlinear analysis and constitutive models of reinforced concrete." *Gihodo-Shuppan Co.*
13) Orakcal, K., Wallace, J. W. and Conte J. P. (2004) "Flexural modeling of reinforced concrete walls-model attributes." *ACI Structural Journal*, No. 101-S68, 688-698.
14) Orakcal, K., Massone, L. M. and Wallace, J. W. (2006) "Analytical modeling of reinforced concrete walls for predicting flexural and coupled-shear-flexural response." *PEER Report 2006/07*, Pacific Earthquake Engineering Research Center.
15) Saito, T., Teshigawara, M., Fukuyama, H., Kato, H., Kusunoki, K., Mukai, T. and Kabeyasawa, T. (2004) "Simulation of nonlinear behavior of reinforced concrete wall-frame structures under earthquake loads." *Proc., 13th World Conference on Earthquake Engineering*, No.1561.
16) Sanada, Y., Kabeyasawa, T. and Nakano, Y. (2004). "Analyses of reinforced concrete wall-frame structural systems considering shear softening of shear wall." *Proc., 13th World Conference on Earthquake Engineering*, No.3036.
17) The 1st, 2nd, 3rd, 4th, and 5th U.S. - Japan workshop on performance-based earthquake engineering methodology for reinforced concrete building structures. (1999-2003). *PEER Report*, Pacific Earthquake Engineering Research Center.
18) The 1st and 2nd NEES/E-Defense workshop on collapse simulation of reinforced concrete building structures. (2005-2006). *PEER Report*, Pacific Earthquake Engineering Research Center.
19) Timoshenko, S. P. and Goodier N. (1970). *Theory of elasticity*, 3rd ed. New York, McGraw-Hill.
20) Vulcano, A. and Bertero, V. V. (1987). "Analytical modeling for predicting the lateral response of reinforced concrete shear walls: evaluation of their reliability." *Report UCB/EERC-87/19*, Earthquake Engineering Research Center, University of California, Berkeley.
21) Vulcano, A., Bertero, V. V. and Colotti, V. (1988). "Analytical modeling of R/C structural walls." *Proc. of 9th World Conference on Earthquake Engineering*, Vol.VI, 41-46.
22) Zienkiewicz, O. C. and Taylor R. L. (2005). *The finite element method for solid and structural mechanics*, 6th ed. Elsevier, Butterworth-Heinemann.
23) Zienkiewicz, O. C., Taylor R. L. and Zhu J. Z. (2005). *The finite element method: Its basis and fundamentals*, 6th ed. Elsevier, Butterworth-Heinemann.

(Submitted: October 9, 2014)
(Accepted: February 6, 2015)